Supplemental Information

RNA Binding and Enzymatic Complexes Constitute the U-Insertion/Deletion Editosome

Inna Aphasizheva[1*], Liye Zhang[2*], Xiaorong Wang[3], Robyn M. Kaake[3], Lan Huang[3], Stefano Monti[2] and Ruslan Aphasizhev[1,#]

Supplemental Figures

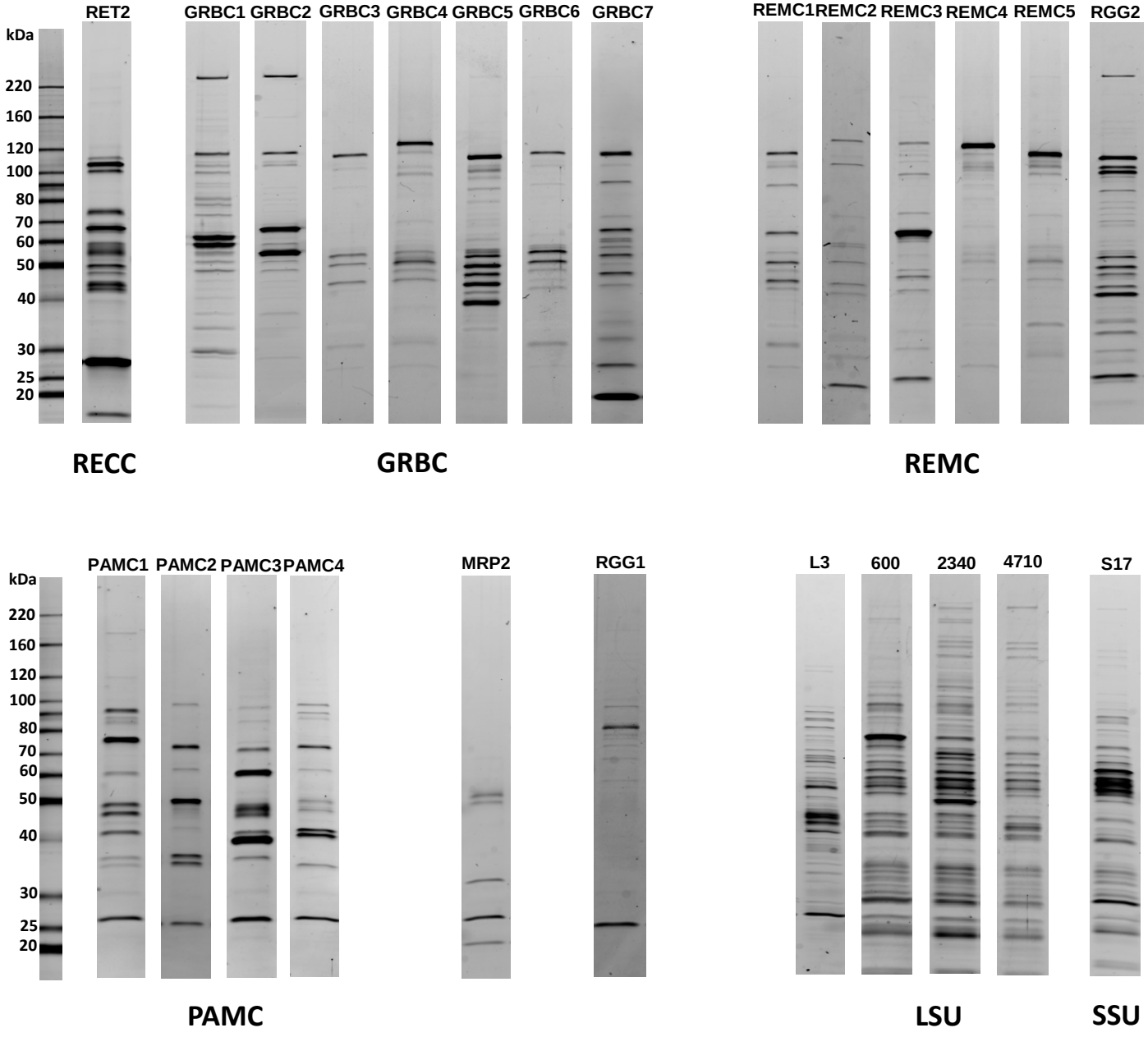
RET2
GRBC1 GRBC2 GRBC3 GRBC4 GRBC5 GRBC6 GRBC7
REMC1 REMC2 REMC3 REMC4 REMC5 RGG2
kDa
220
160
120
100
80
70
60
50
40
30
25
20
RECC
GRBC
REMC
PAMC1 PAMC2 PAMC3 PAMC4
MRP2
RGG1
L3
600
2340
4710
S17
PAMC
LSU
SSU

Supplemental Figure S1. Representative tandem affinity purifications of RNA processing complexes from mitochondria of *Trypanosoma brucei.* Final fractions were separated on 8%–16% SDS gradient gels and stained with Sypro Ruby. LSU–large ribosomal subunit; SSU–small ribosomal subunit.

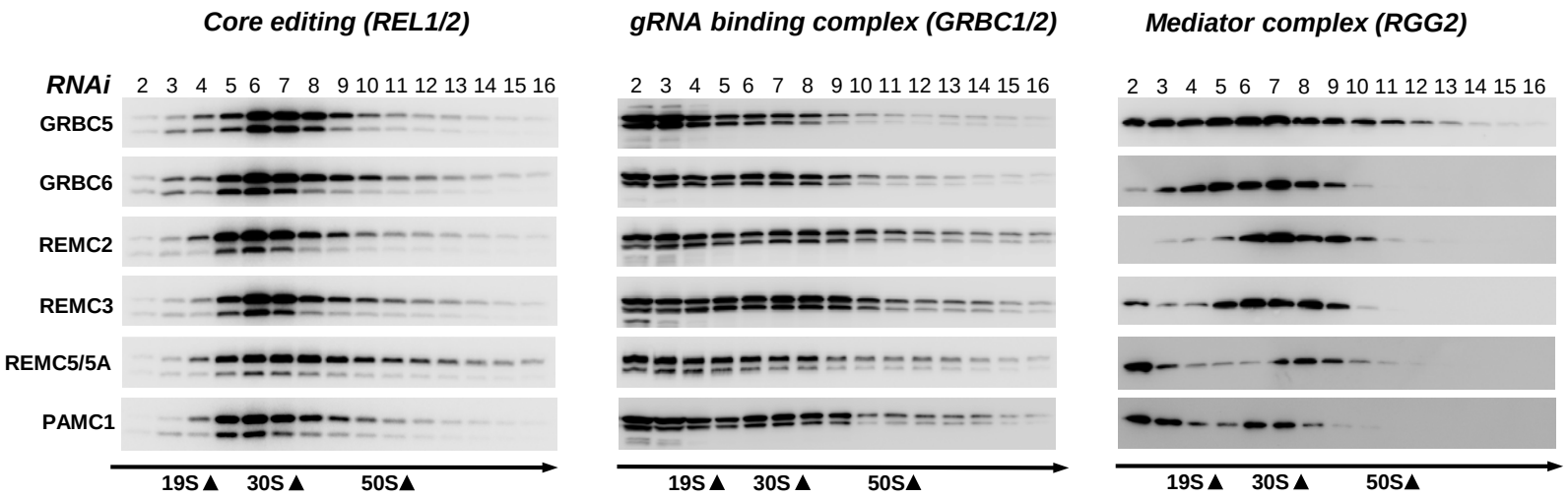
Core editing (REL1/2)
gRNA binding complex (GRBC1/2)
Mediator complex (RGG2)
RNAi
2 3 4 5 6 7 8 9 10 11 12 13 14 15 16
GRBC5
GRBC6
REMC2
REMC3
REMC5/5A
PAMC1
19S▲ 30S▲ 50S▲

Supplemental Figure S2. Sedimentation patterns of RNA editing core (RECC), gRNA binding (GRBC) and RNA editing mediator (REMC). Gradient fractions were incubated with [a–^{32}P]ATP to produce self-adenylated RNA editing ligases REL1 and REL2, separated on 8%–16% gradient SDS gels, transferred onto nitrocellulose membrane, exposed to phosphor storage screen, and sequentially probed with antibodies against RGG2, MERS1 and GRBC1/2.

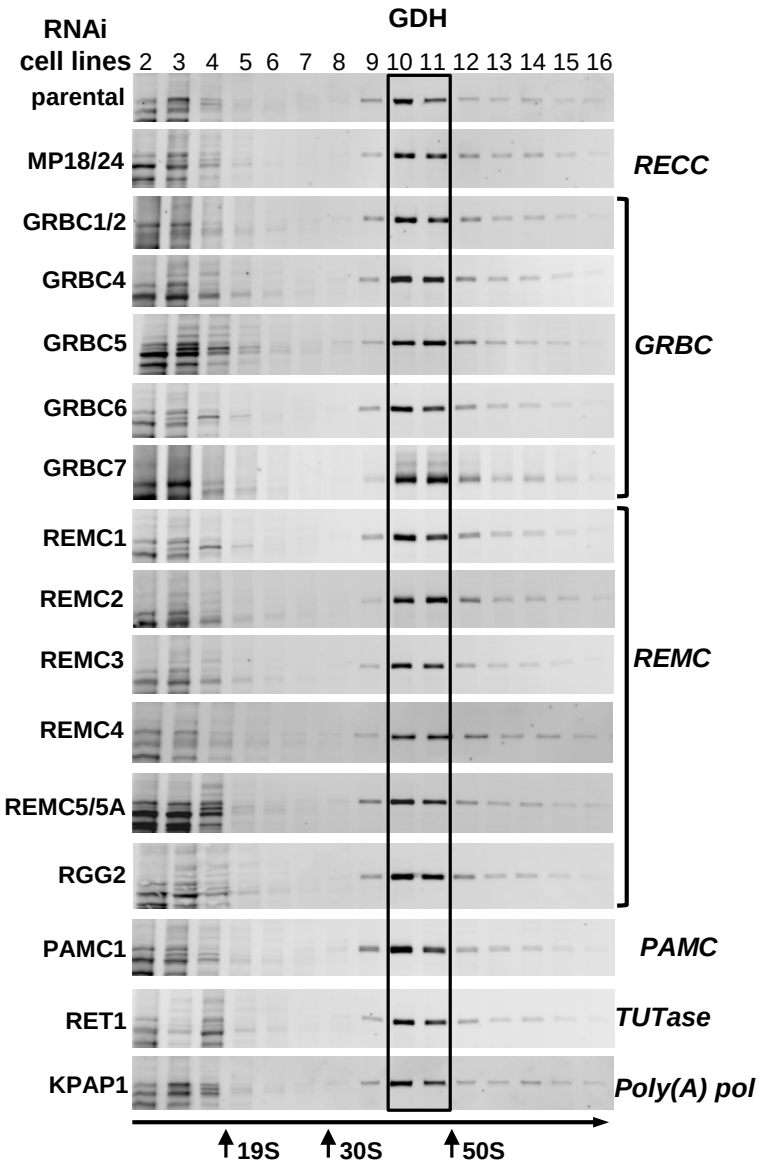
RNAi cell lines
GDH
2 3 4 5 6 7 8 9 10 11 12 13 14 15 16
parental
MP18/24
RECC
GRBC1/2
GRBC4
GRBC5
GRBC6
GRBC7
GRBC
REMC1
REMC2
REMC3
REMC4
REMC5/5A
RGG2
REMC
PAMC1
PAMC
RET1
TUTase
KPAP1
Poly(A) pol
19S
30S
50S

Supplemental Figure S3. Glycerol gradient fractionation of mitochondrial extracts.

Fractions were separated on 8%–16% gradient SDS gels, transferred onto nitrocellulose membrane and stained with Sypro Ruby. Consistency of glycerol gradients was assessed by sedimentation patters of glutamate dehydrogenase, GDH.

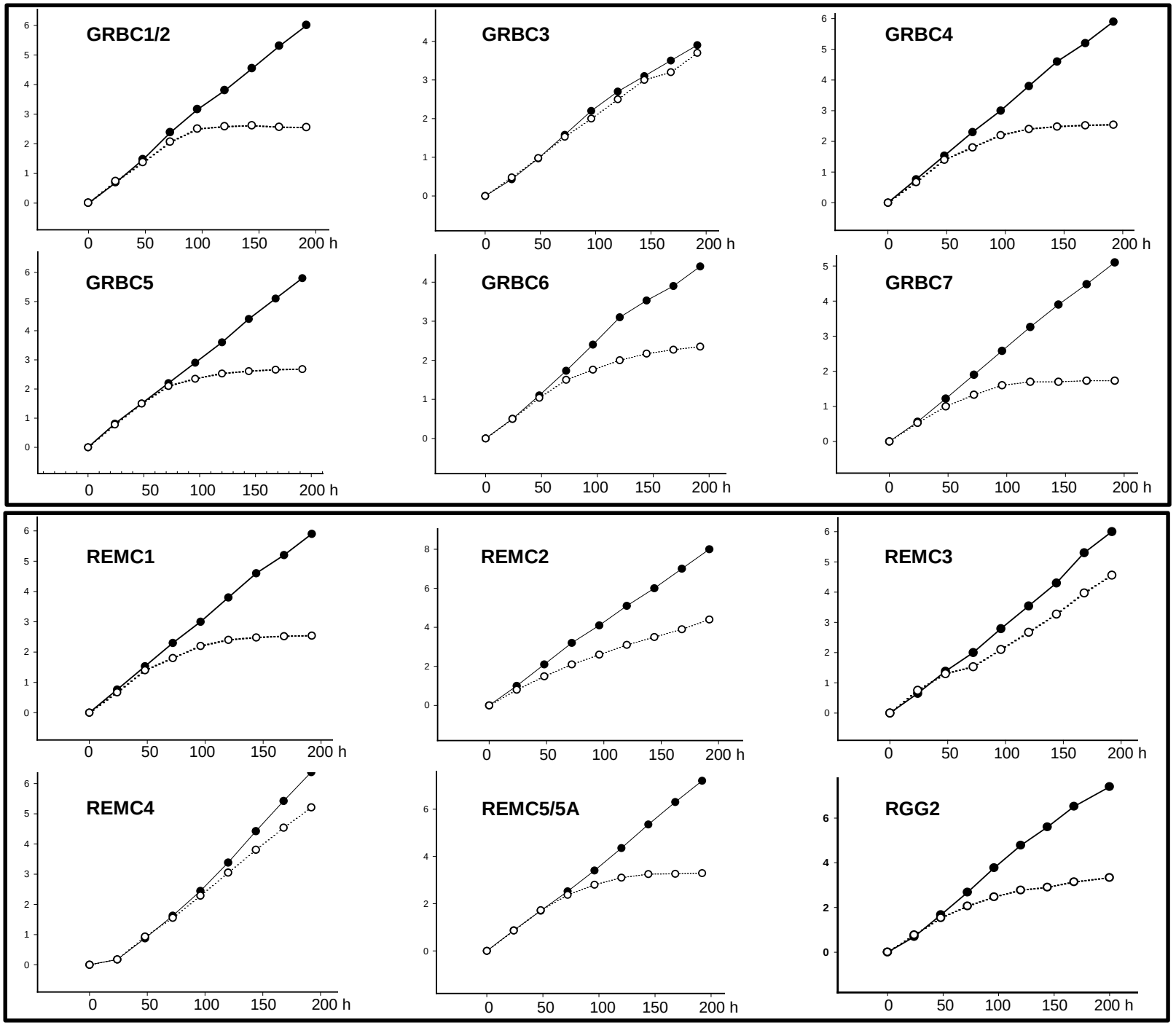
GRBC
GRBC1/2
GRBC3
GRBC4
GRBC5
GRBC6
GRBC7
REMC
REMC1
REMC2
REMC3
REMC4
REMC5/5A
RGG2
0 50 100 150 200 h

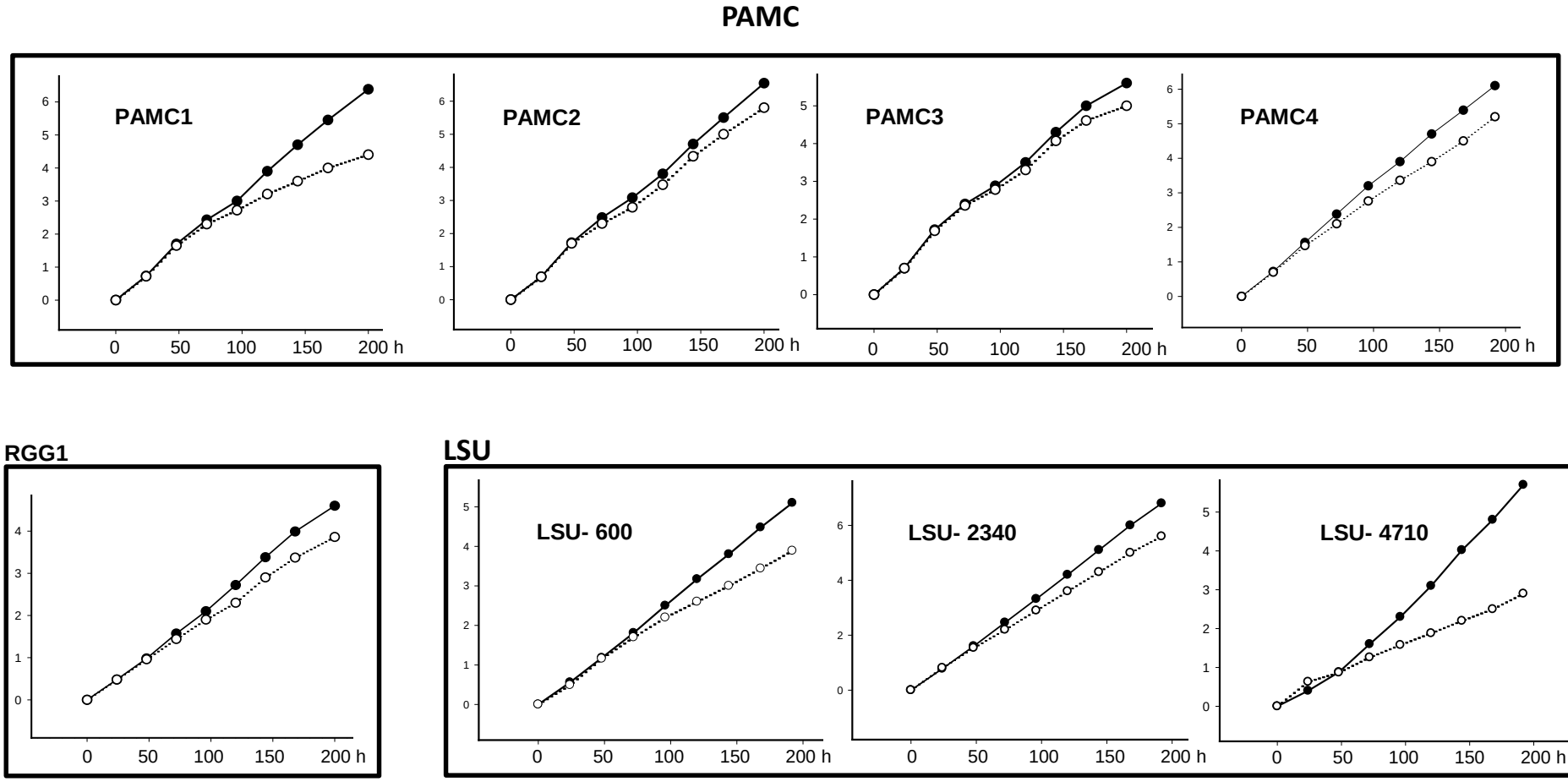
PAMC
PAMC1
PAMC2
PAMC3
PAMC4
RGG1
LSU
LSU- 600
LSU- 2340
LSU- 4710
0
50
100
150
200 h

Supplemental Figure S4. Growth kinetics of procyclic parasite cultures after mock (closed circles) or RNAi induction (open circles). Cumulative cell count (log) was plotted against RNAi induction time.

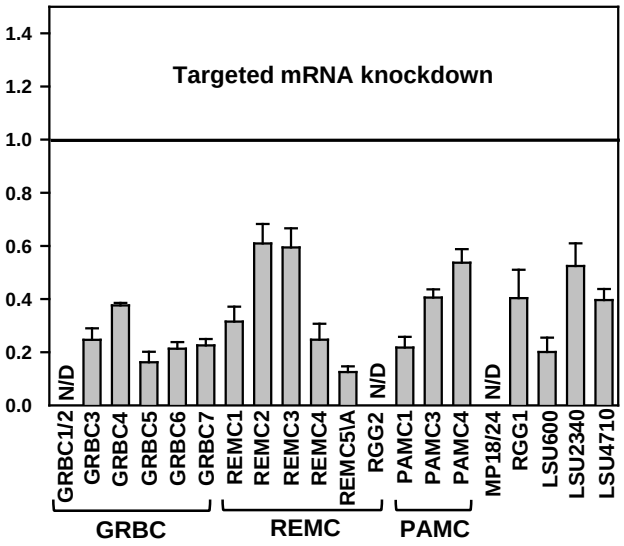
Targeted mRNA knockdown
1.4
1.2
1.0
0.8
0.6
0.4
0.2
0.0
N/D
N/D
N/D
GRBC1/2
GRBC3
GRBC4
GRBC5
GRBC6
GRBC7
REMC1
REMC2
REMC3
REMC4
REMC5\A
RGG2
PAMC1
PAMC3
PAMC4
MP18/24
RGG1
LSU600
LSU2340
LSU4710
GRBC
REMC
PAMC

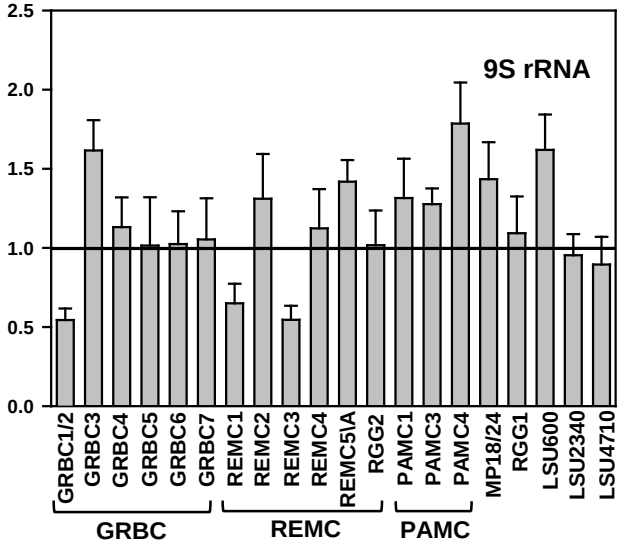
9S rRNA
2.5
2.0
1.5
1.0
0.5
0.0
GRBC1/2
GRBC3
GRBC4
GRBC5
GRBC6
GRBC7
REMC1
REMC2
REMC3
REMC4
REMC5\A
RGG2
PAMC1
PAMC3
PAMC4
MP18/24
RGG1
LSU600
LSU2340
LSU4710
GRBC
REMC
PAMC

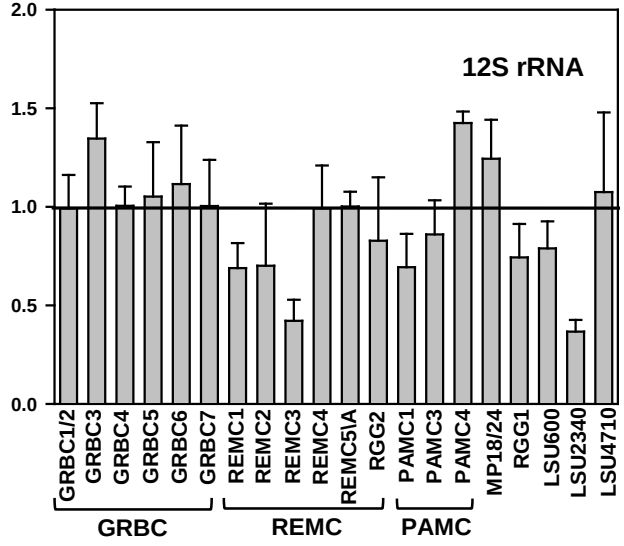
12S rRNA
2.0
1.5
1.0
0.5
0.0
GRBC1/2
GRBC3
GRBC4
GRBC5
GRBC6
GRBC7
REMC1
REMC2
REMC3
REMC4
REMC5\A
RGG2
PAMC1
PAMC3
PAMC4
MP18/24
RGG1
LSU600
LSU2340
LSU4710
GRBC
REMC
PAMC

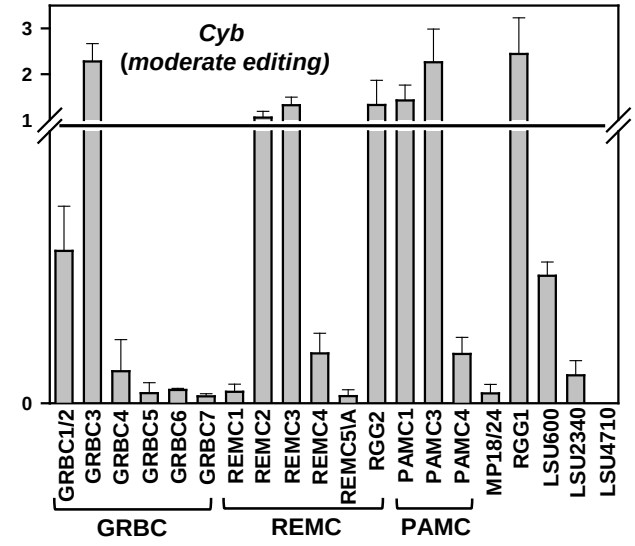
Cyb
(moderate editing)
3
2
1
0
GRBC1/2
GRBC3
GRBC4
GRBC5
GRBC6
GRBC7
REMC1
REMC2
REMC3
REMC4
REMC5\A
RGG2
PAMC1
PAMC3
PAMC4
MP18/24
RGG1
LSU600
LSU2340
LSU4710
GRBC
REMC
PAMC

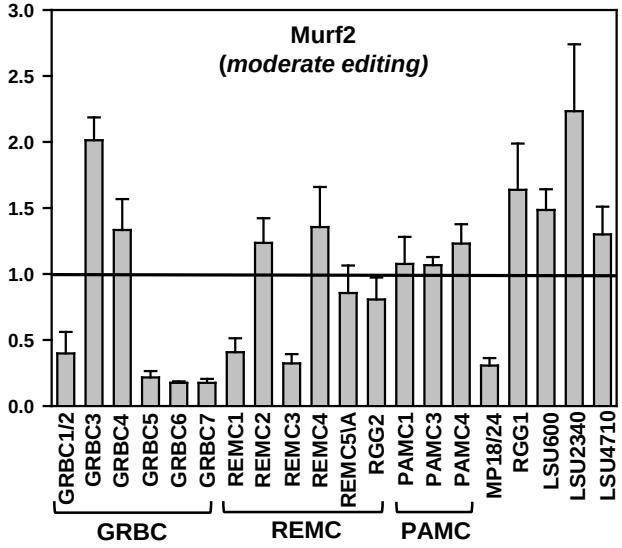
Murf2
(moderate editing)
3.0
2.5
2.0
1.5
1.0
0.5
0.0
GRBC1/2
GRBC3
GRBC4
GRBC5
GRBC6
GRBC7
REMC1
REMC2
REMC3
REMC4
REMC5\A
RGG2
PAMC1
PAMC3
PAMC4
MP18/24
RGG1
LSU600
LSU2340
LSU4710
GRBC
REMC
PAMC

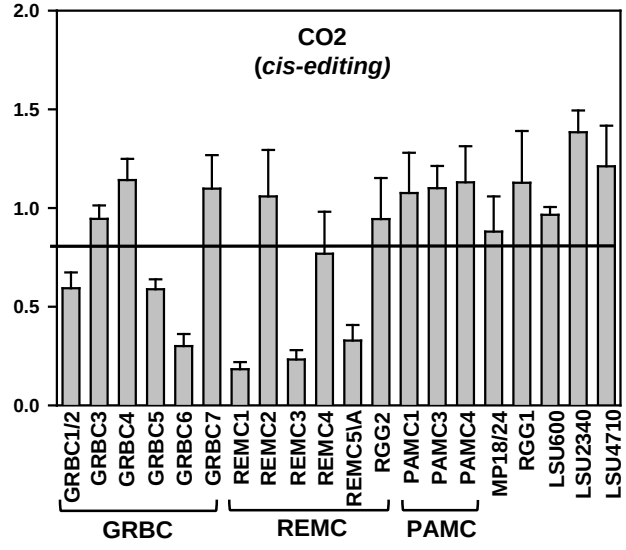
CO2
(cis-editing)
2.0
1.5
1.0
0.5
0.0
GRBC1/2
GRBC3
GRBC4
GRBC5
GRBC6
GRBC7
REMC1
REMC2
REMC3
REMC4
REMC5\A
RGG2
PAMC1
PAMC3
PAMC4
MP18/24
RGG1
LSU600
LSU2340
LSU4710
GRBC
REMC
PAMC

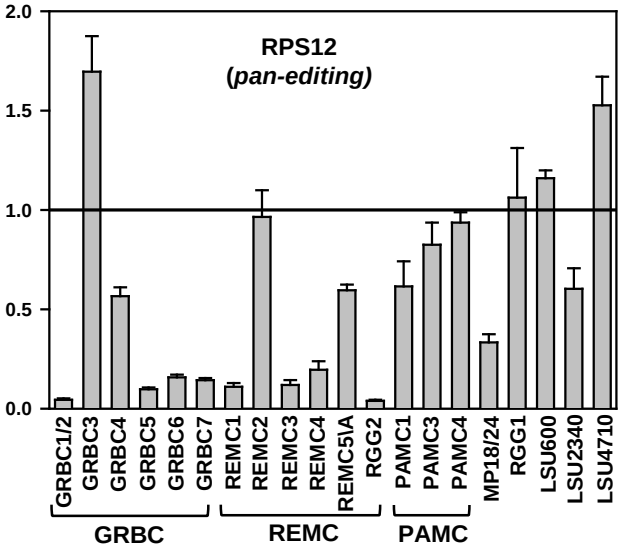
RPS12
(pan-editing)
2.0
1.5
1.0
0.5
0.0
GRBC1/2
GRBC3
GRBC4
GRBC5
GRBC6
GRBC7
REMC1
REMC2
REMC3
REMC4
REMC5\A
RGG2
PAMC1
PAMC3
PAMC4
MP18/24
RGG1
LSU600
LSU2340
LSU4710
GRBC
REMC
PAMC

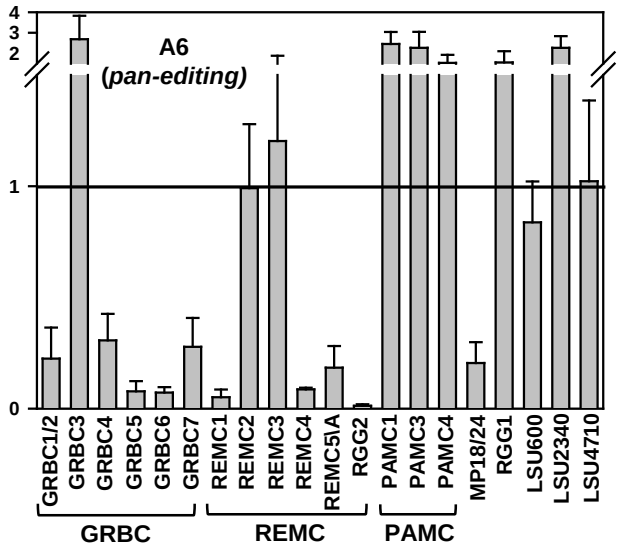
A6
(pan-editing)
4
3
2
1
0
GRBC1/2
GRBC3
GRBC4
GRBC5
GRBC6
GRBC7
REMC1
REMC2
REMC3
REMC4
REMC5\A
RGG2
PAMC1
PAMC3
PAMC4
MP18/24
RGG1
LSU600
LSU2340
LSU4710
GRBC
REMC
PAMC

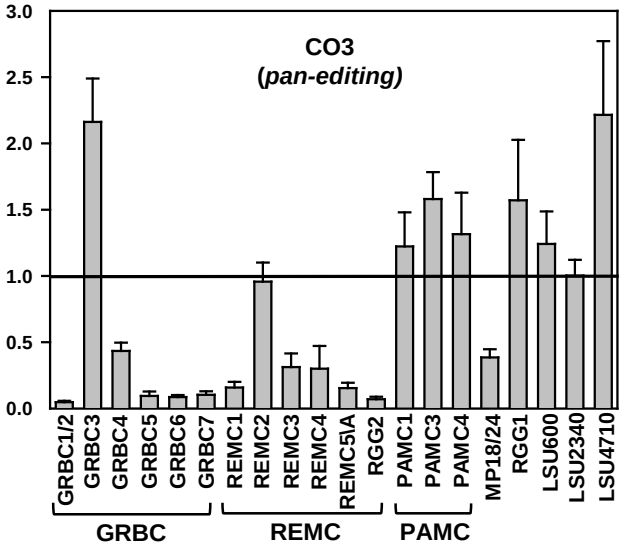
CO3
(pan-editing)
3.0
2.5
2.0
1.5
1.0
0.5
0.0
GRBC1/2
GRBC3
GRBC4
GRBC5
GRBC6
GRBC7
REMC1
REMC2
REMC3
REMC4
REMC5\A
RGG2
PAMC1
PAMC3
PAMC4
MP18/24
RGG1
LSU600
LSU2340
LSU4710
GRBC
REMC
PAMC

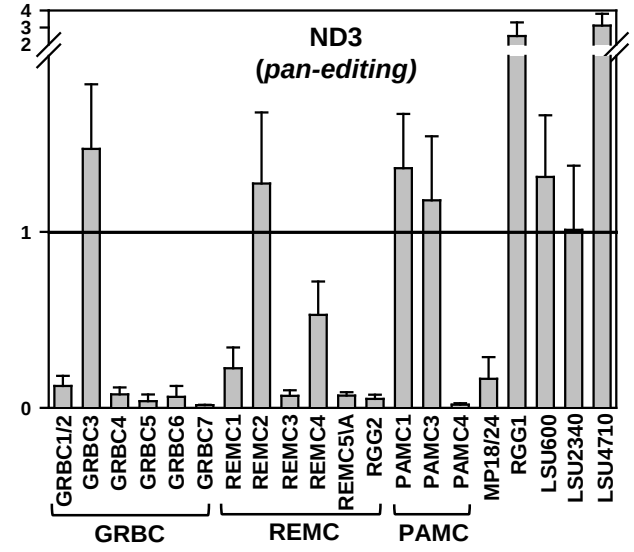
ND3
(pan-editing)
4
3
2
1
0
GRBC1/2
GRBC3
GRBC4
GRBC5
GRBC6
GRBC7
REMC1
REMC2
REMC3
REMC4
REMC5\A
RGG2
PAMC1
PAMC3
PAMC4
MP18/24
RGG1
LSU600
LSU2340
LSU4710
GRBC
REMC
PAMC

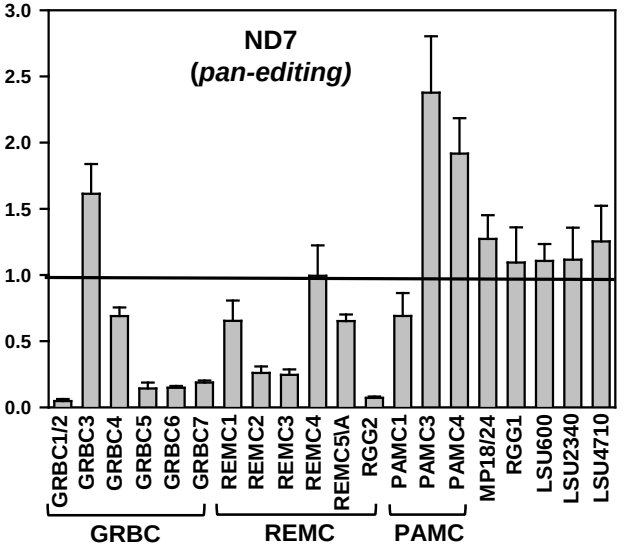
ND7
(pan-editing)
3.0
2.5
2.0
1.5
1.0
0.5
0.0
GRBC1/2
GRBC3
GRBC4
GRBC5
GRBC6
GRBC7
REMC1
REMC2
REMC3
REMC4
REMC5\A
RGG2
PAMC1
PAMC3
PAMC4
MP18/24
RGG1
LSU600
LSU2340
LSU4710
GRBC
REMC
PAMC

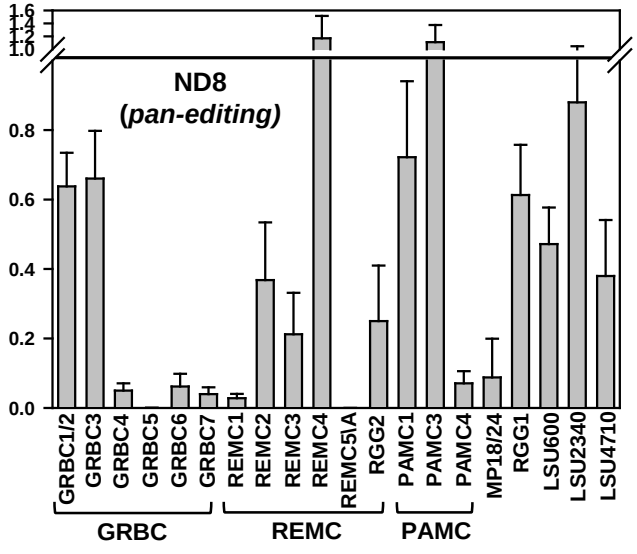
ND8
(pan-editing)
1.6
1.4
1.2
1.0
0.8
0.6
0.4
0.2
0.0
GRBC1/2
GRBC3
GRBC4
GRBC5
GRBC6
GRBC7
REMC1
REMC2
REMC3
REMC4
REMC5\A
RGG2
PAMC1
PAMC3
PAMC4
MP18/24
RGG1
LSU600
LSU2340
LSU4710
GRBC
REMC
PAMC

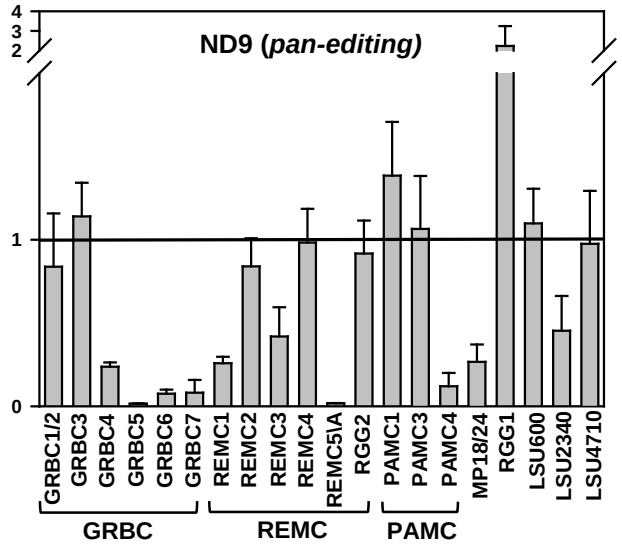
ND9 (*pan-editing*)
4
3
2
1
0
GRBC1/2
GRBC3
GRBC4
GRBC5
GRBC6
GRBC7
REMC1
REMC2
REMC3
REMC4
REMC5\A
RGG2
PAMC1
PAMC3
PAMC4
MP18/24
RGG1
LSU600
LSU2340
LSU4710
GRBC
REMC
PAMC

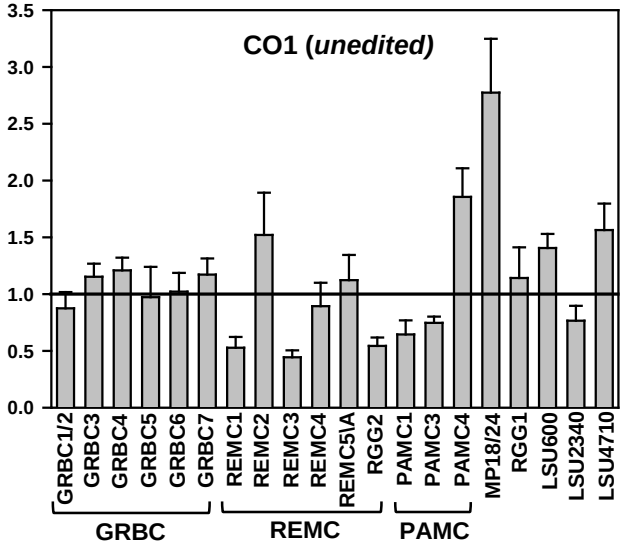
CO1 (*unedited*)
3.5
3.0
2.5
2.0
1.5
1.0
0.5
0.0
GRBC1/2
GRBC3
GRBC4
GRBC5
GRBC6
GRBC7
REMC1
REMC2
REMC3
REMC4
REMC5\A
RGG2
PAMC1
PAMC3
PAMC4
MP18/24
RGG1
LSU600
LSU2340
LSU4710
GRBC
REMC
PAMC

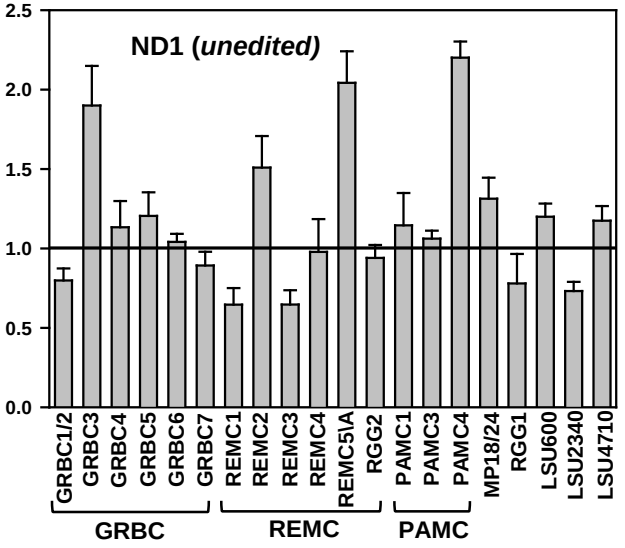
ND1 (*unedited*)
2.5
2.0
1.5
1.0
0.5
0.0
GRBC1/2
GRBC3
GRBC4
GRBC5
GRBC6
GRBC7
REMC1
REMC2
REMC3
REMC4
REMC5\A
RGG2
PAMC1
PAMC3
PAMC4
MP18/24
RGG1
LSU600
LSU2340
LSU4710
GRBC
REMC
PAMC

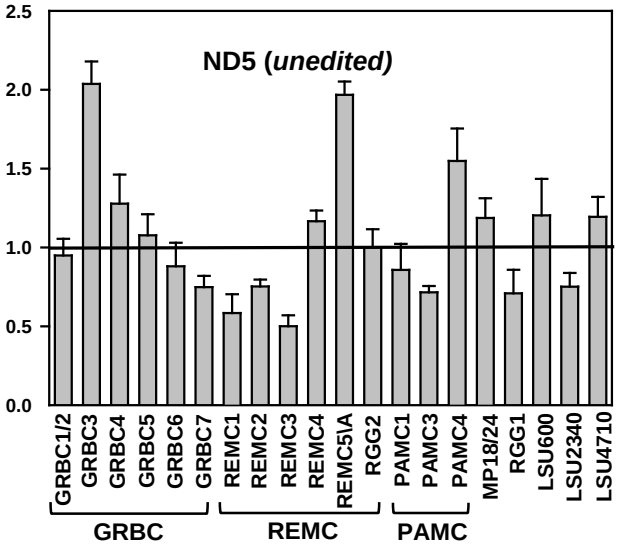
ND5 (*unedited*)
2.5
2.0
1.5
1.0
0.5
0.0
GRBC1/2
GRBC3
GRBC4
GRBC5
GRBC6
GRBC7
REMC1
REMC2
REMC3
REMC4
REMC5\A
RGG2
PAMC1
PAMC3
PAMC4
MP18/24
RGG1
LSU600
LSU2340
LSU4710
GRBC
REMC
PAMC

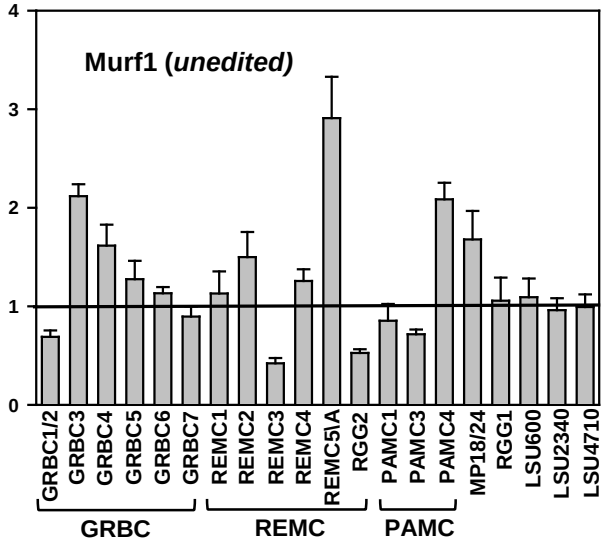
Murf1 (*unedited*)
4
3
2
1
0
GRBC1/2
GRBC3
GRBC4
GRBC5
GRBC6
GRBC7
REMC1
REMC2
REMC3
REMC4
REMC5\A
RGG2
PAMC1
PAMC3
PAMC4
MP18/24
RGG1
LSU600
LSU2340
LSU4710
GRBC
REMC
PAMC

Supplemental Figure S5. Quantitative real-time RT-PCR analysis of RNAi-targeted nuclear mRNAs, and mitochondrial rRNAs, edited and unedited mRNAs in respective RNAi knockdowns

RNA levels were normalized to β-tubulin mRNA. RNAi was induced for 72 hours. Error bars represent the standard deviation from at least three replicates. The thick line at ‘‘1’’ reflects no change in relative abundance upon RNAi induction; bars above or below represent an increase or decrease, respectively. N/D: not determined.

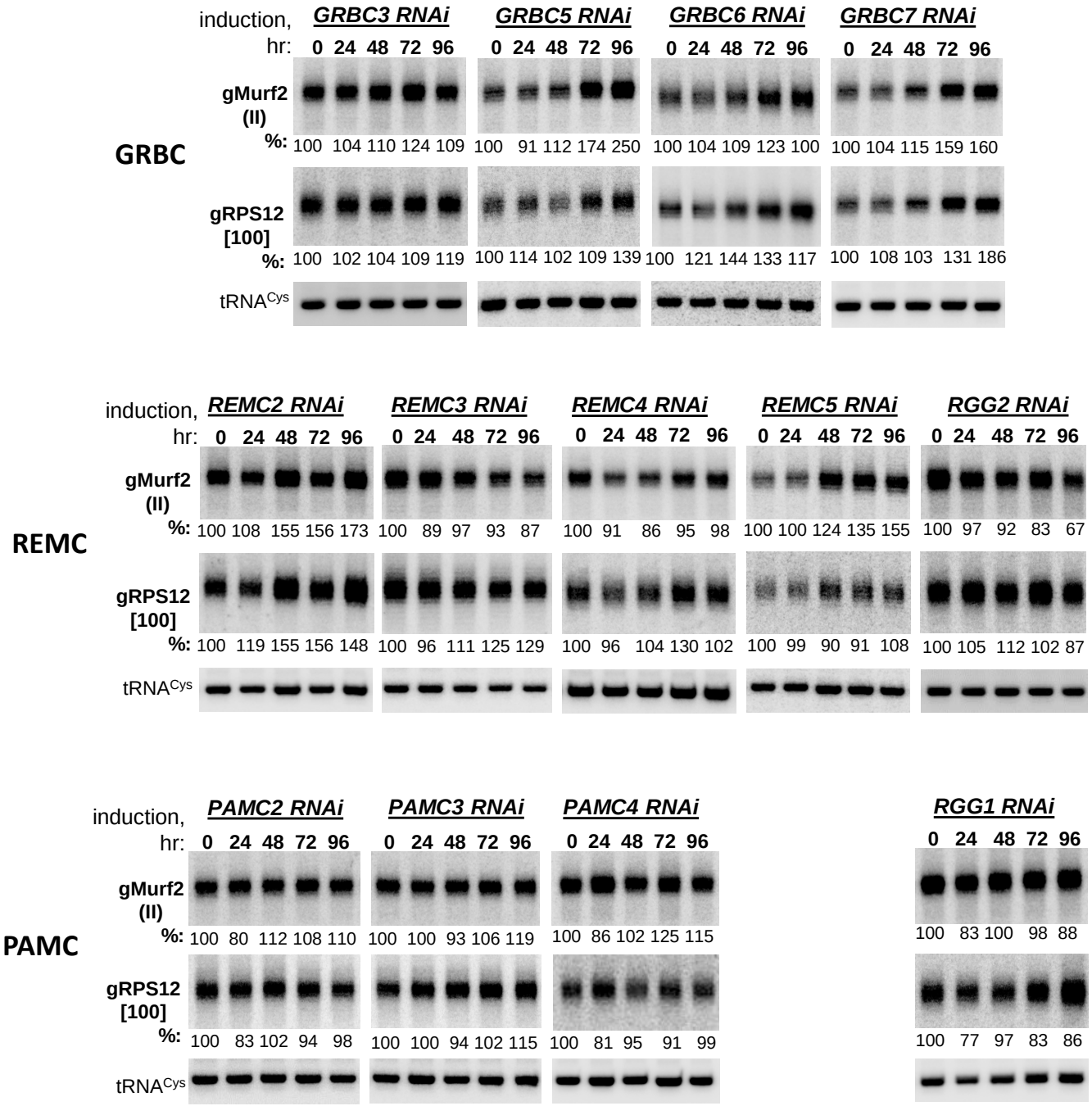
induction,
hr:
GRBC3 RNAi
GRBC5 RNAi
GRBC6 RNAi
GRBC7 RNAi
0 24 48 72 96
GRBC
gMurf2 (II)
%: 100 104 110 124 109 100 91 112 174 250 100 104 109 123 100 100 104 115 159 160
gRPS12 [100]
%: 100 102 104 109 119 100 114 102 109 139 100 121 144 133 117 100 108 103 131 186
tRNACys
REMC
REMC2 RNAi
REMC3 RNAi
REMC4 RNAi
REMC5 RNAi
RGG2 RNAi
gMurf2 (II)
%: 100 108 155 156 173 100 89 97 93 87 100 91 86 95 98 100 100 124 135 155 100 97 92 83 67
gRPS12 [100]
%: 100 119 155 156 148 100 96 111 125 129 100 96 104 130 102 100 99 90 91 108 100 105 112 102 87
tRNACys
PAMC
PAMC2 RNAi
PAMC3 RNAi
PAMC4 RNAi
RGG1 RNAi
gMurf2 (II)
%: 100 80 112 108 110 100 100 93 106 119 100 86 102 125 115 100 83 100 98 88
gRPS12 [100]
%: 100 83 102 94 98 100 100 94 102 115 100 81 95 91 99 100 77 97 83 86
tRNACys

Supplemental Figure S6. Northern blotting analysis of RNAi-induced changes in guide RNA abundance. Total RNA was isolated at indicated time points after RNAi induction. Relative gRNA abundance was calculated in reference to the nuclear-encoded but mitochondrion-localized $tRNA^{Cys}$.

RPS12 (pan-editing)

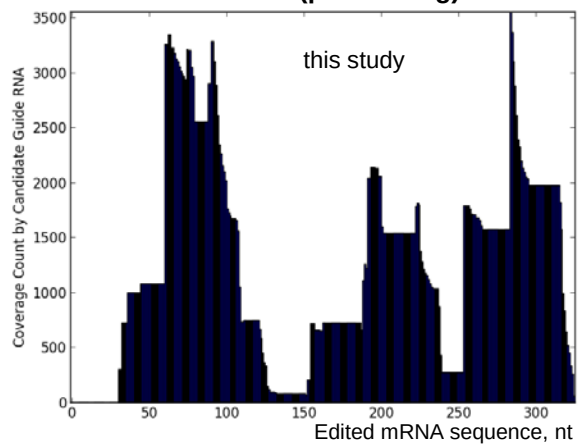

A6 (pan-editing)

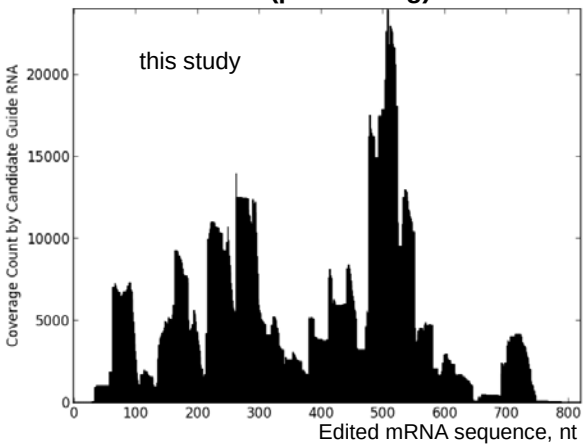

CO3 (pan-editing)

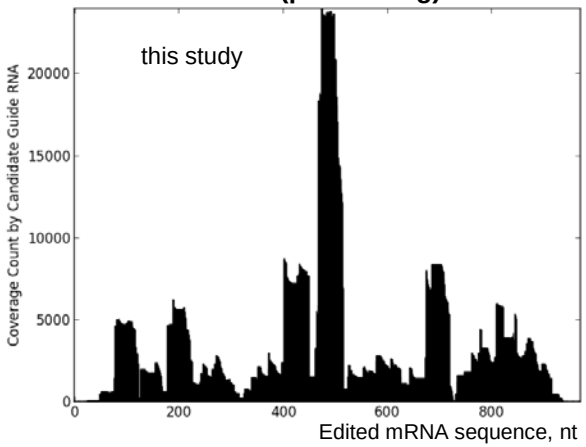

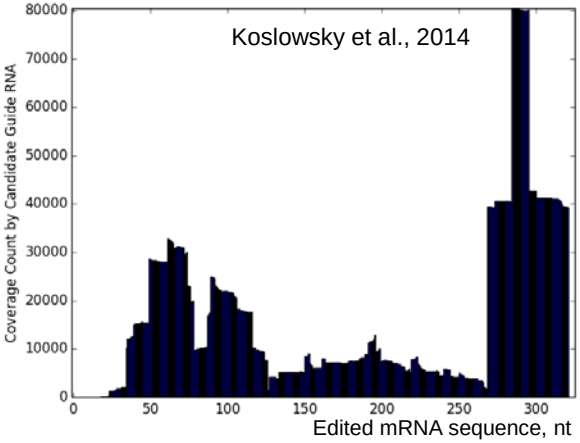

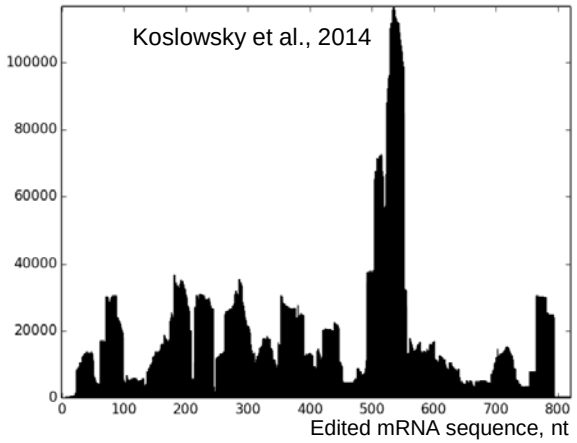

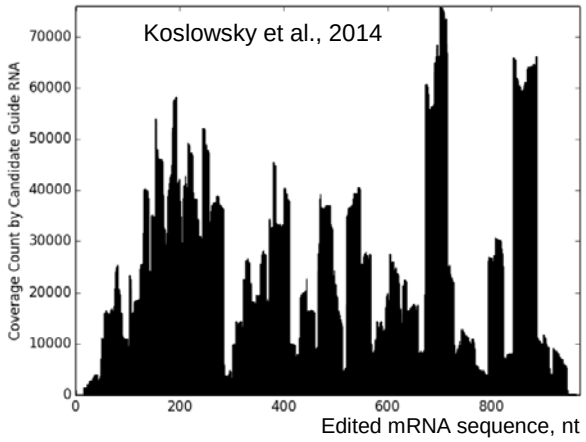

Cyb (moderate editing at 5' region)

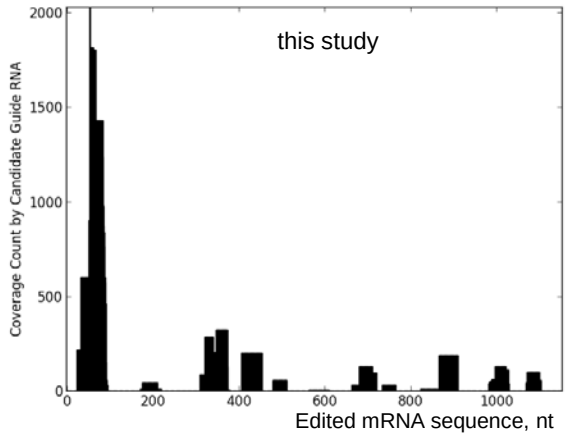

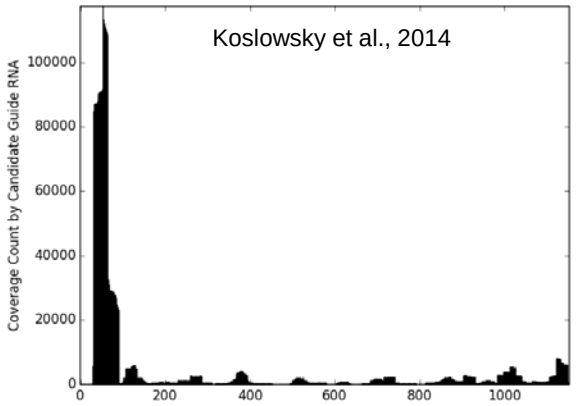

CO2 (*cis*-editing)

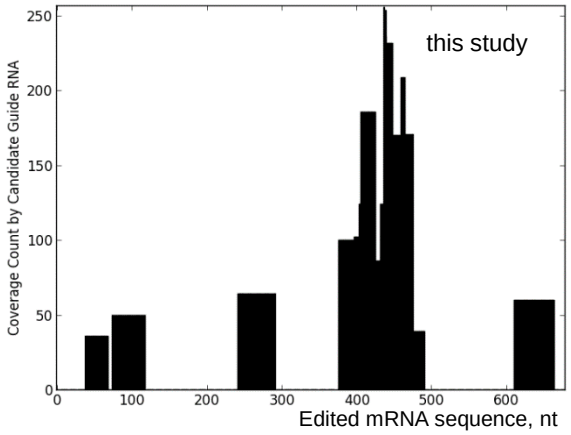

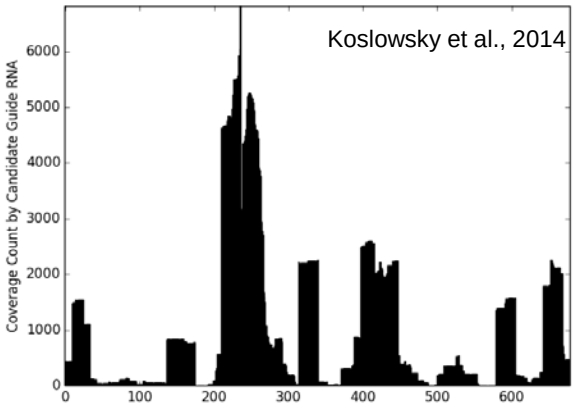

Supplemental Figure S7. Coverage of pan-edited (RPS12, A6 and CO3), moderately edited (cyb) and *cis*-edited mRNA (CO2) by candidate gRNAs. Messenger RNA coverage by candidate gRNA raw read counts was computed for each mRNA nucleotide. Custom scripts developed for this study are compared to those used by (Koslowsky et al., 2013).

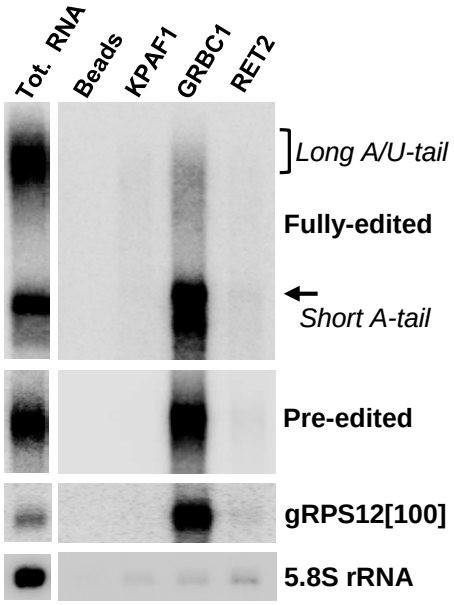
Tot. RNA
Beads
KPAF1
GRBC1
RET2
Long A/U-tail
Fully-edited
Short A-tail
Pre-edited
gRPS12[100]
5.8S rRNA

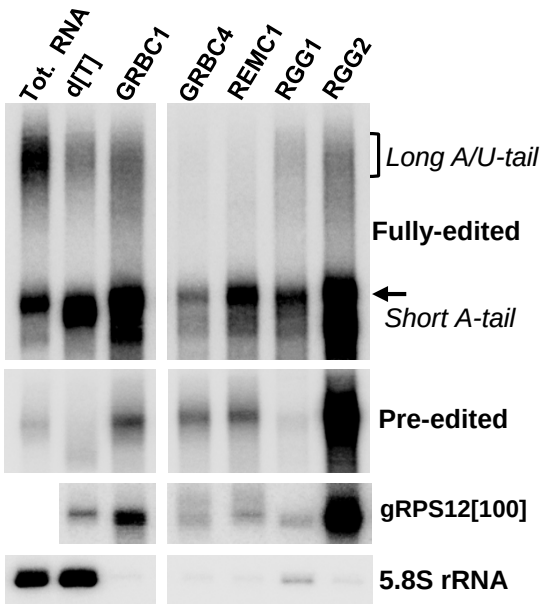
Tot. RNA
d[T]
GRBC1
GRBC4
REMC1
RGG1
RGG2
Long A/U-tail
Fully-edited
Short A-tail
Pre-edited
gRPS12[100]
5.8S rRNA

Figure S8. Distribution of pre-edited, fully-edited mRNAs and guide RNAs among complexes. RNA was extracted from magnetic beads, separated on 5% polyacrylamide/8M urea gel and probed for respective mRNA species. [dT], total RNA was treated with RNase H in the presence of 18-mer [dT] to remove poly(A) tails. Beads, IgG-coated magnetic beads were incubated with extract from the parental cell line.

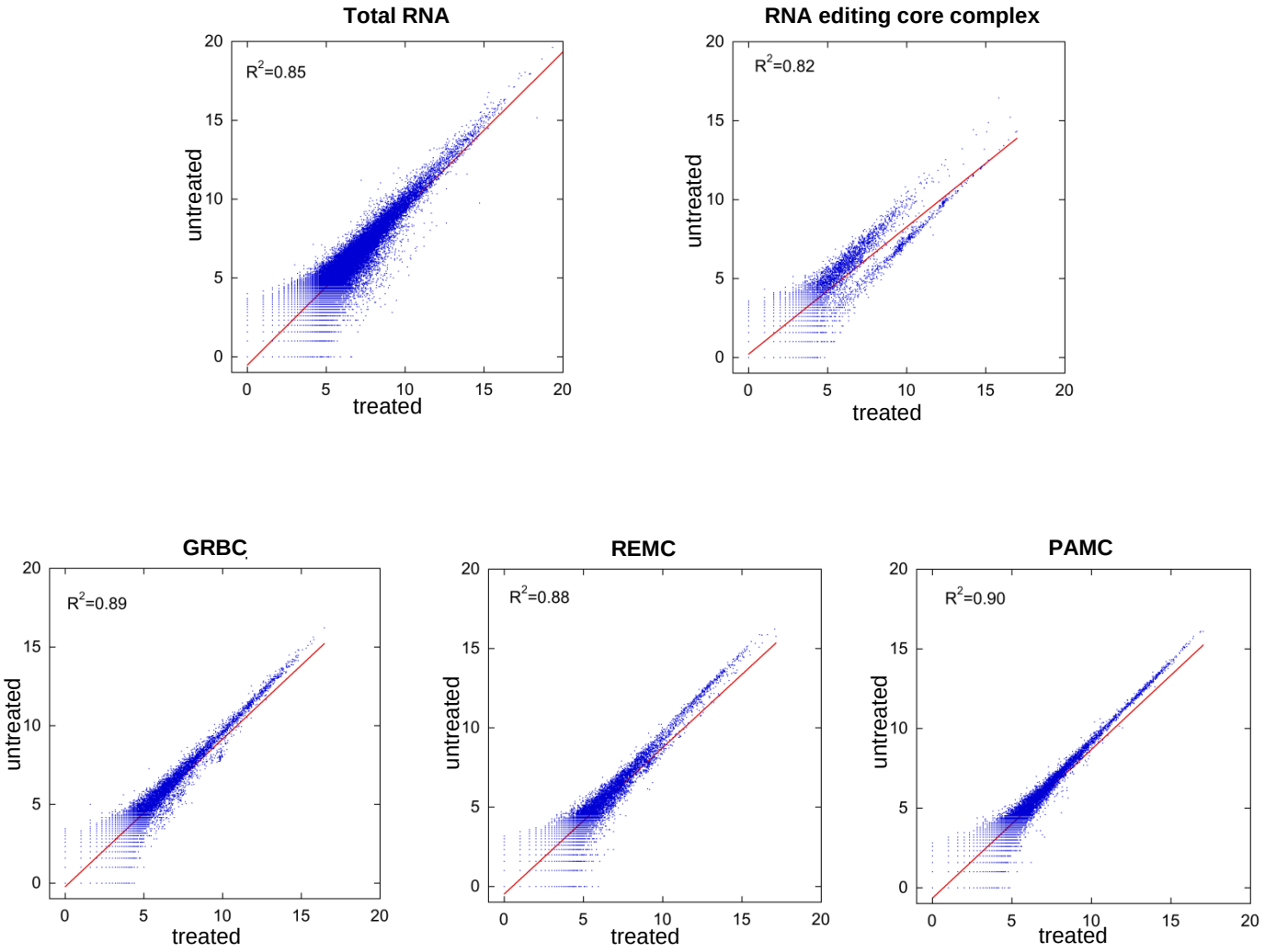
Total RNA
R2=0.85
RNA editing core complex
R2=0.82
GRBC
R2=0.89
REMC
R2=0.88
PAMC
R2=0.90
untreated
treated
0
5
10
15
20

Figure S9. Similarity of small RNA libraries obtained from mock and Terminator exonuclease-treated samples. Pearson correlation coefficient was calculated for mock- and Terminator exonuclease-treated small RNA samples extracted from purified mitochondrial fraction and affinity purified complexes. The $\log_2$ transformed read counts for each transcript were plotted.

Supplemental experimental procedures

Mitochondrial Isolation, Glycerol Gradients, Immunoprecipitation, Affinity Purification and Western Blotting

Mitochondrial fraction was isolated as described except omitting the Percoll density gradient(Pelletier et al., 2007). Fresh mitochondrial pellets were mixed with three parts (wet weight) of buffer containing 25 mM HEPES (pH 7.6), 125 mM KCl, 12 mM $MgCl_2$ and 1.2 % Nonidet P-40 (NP-40). After 10 minutes of incubation on ice, the extract was clarified at 18,000 g for 10 min and fractionated on 10%-30% glycerol gradient in SW41 rotor for 4 hours at 178,000 g and 580 μl fractions were collected from the top. Self-adenylation of RNA ligases was carried out with 1 μCi of [-^{32}P]ATP per 10 μl of gradient fraction. Western blotting was performed with rabbit antigen-purified polyclonal antibodies or with anti-CBP antibodies (GenScript) to detect tagged proteins. Affinity pulldowns were performed with 5 μl of protein G agarose beads (GE Healthcare) coated with antigen-purified antibodies in the presence of 1 mg/ml of albumin and 0.2% of NP-40. Beads were washed three times for 10 min in the extraction buffer with 0.2 % NP-40. RNA was extracted from beads with phenol/chloroform and precipitated. Quantitative chemiluminescent images were acquired with LAS-4000 digital analyzer (Fuji). The conventional TAP procedure was performed as described except that all buffers contained 100 mM KCl and 1 mM EDTA (Aphasizhev and Aphasizheva, 2007). For the rapid pulldown, rabbit IgG was coupled to Dynabeads M-270 Epoxy (Invitrogen) and used in total cell extract (Aphasizheva et al., 2011).

RNA Analysis

Northern blotting, guanylyltransferase labeling and qRT-PCR were performed as previously described (Aphasizheva et al., 2011). For RNA-Seq, RNA was extracted from Renografin density gradient-purified mitochondrial fraction or from rapid affinity purified complexes and separated on 10% PAGE with 8M urea. RNA was excised from areas corresponding to 35-75 nt, eluted and processed with ScriptMiner™ Small RNA-Seq Library Preparation Kit to generate Illumina-compatible libraries as recommended by manufacturer (Epicentre). Single-read 75 nt stranded sequencing and raw data extraction were performed at the UC Irvine Genomics High-Throughput Facility.

LC MS/MS analysis

Affinity-purified complexes were precipitated by addition of trichloroacetic acid and deoxycholate to 20% and 0.1%, respectively, washed three times with ice-cold acetone and digested with 2% (w/w) LysC peptidase in 8M urea for 4 hours at 37^0C. Reaction was diluted five-fold with 50 mM ammonium bicarbonate and further digested with 1% trypsin (w:w) for 16 hours. Peptides were purified on Vivapure spin columns (Sartorius). LC MS/MS was carried out by nanoflow reverse phase liquid chromatography (RPLC) (Eksigent, CA) coupled on-line to a Linear Ion Trap (LTQ)-Orbitrap XL mass spectrometer (Thermo Scientific) as described(Fang et al., 2012). The LC analysis was performed using a capillary column (100 μm ID x 150 mm long) packed with Inertsil ODS-3 resin (GL Sciences) and the peptides were eluted using a linear gradient of 2% to 35% B in 85 min at a flow of 400 nL/min (solvent A: 100% H_2O/0.1% formic

acid; solvent B: 100 % acetonitrile/0.1% formic acid). A cycle of one full FT scan mass spectrum (350-1800 m/z, resolution of 60,000 at m/z 400) followed by ten data-dependent MS/MS scans was acquired in the linear ion trap with normalized collision energy (setting of 35%). Target ions already selected for MS/MS were dynamically excluded for 30 s.

Protein identification by database searching

Monoisotopic masses of parent ions and corresponding fragment ions, parent ion charge states and ion intensities from the tandem mass spectra (MS/MS) were obtained by using in-house software with Raw_Extract script from Xcalibur v2.4. Following automated data extraction, resultant peak lists for each LC MS/MS experiment were submitted to the development version of Protein Prospector (UCSF) for database searching as described(Kaake et al., 2010). Each project was searched against a normal form concatenated with the random form of the *T. brucei* database (www.genedb.org, v5). Trypsin was set as the enzyme with a maximum of two missed cleavage sites. The mass tolerance for parent ion was set as ±20 ppm, whereas ±0.6 Da tolerance was chosen for the fragment ions. Chemical modifications such as protein N-terminal acetylation, methionine oxidation, N-terminal pyroglutamine, and deamidation of asparagine were selected as variable modifications during database search. The Search Compare program in Protein Prospector was used for summarization, validation and comparison of results. Protein identification was based on at least three unique peptides with expectation value ≤0.05.

Calculation of distributed normalized spectral abundance factor (dNSAF)

We have utilized a label-free quantification strategy developed by Washburn and colleagues(Zhang et al., 2010), which makes use of the quantitative information stored in MS/MS data as spectral counts, and converts peptide counts into a normalized value, the distributed normalized spectral abundance factor (dNSAF), for subsequent quantitation. Using an in-house generated analysis platform (Fang et al., 2012), we calculated the dNSAF for each putative interactor in each bait purification. Total unique and shared peptide counts were calculated from the peptide report generated from Search Compare in Protein Prospector (v 5.8.0) and analyzed as described (Fang et al., 2012). The dNSAF values of proteins identified from all experiments are reported in Supplemental Table 1.

Generation of protein-protein interaction network and heatmaps

The interaction network was generated from bait-prey pairs in which the prey protein was identified with at least 4 unique peptides (Supplemental table 1). The resulting network map was generated from an excel file detailing source (bait), target (prey), interaction type (pp), and interaction strength (dNSAF) which was then visualized with Cytoscape software (http://www.cytoscape.org). In the interaction network, each node represents a single bait or prey protein and every edge represents an identified interaction. The edge thickness and color intensity correlate with dNSAF values. To simplify the interaction network, reciprocal interactions (i.e. bait-bait interactions captured in both purifications) were shown by a single edge for which the interaction strength was represented by the sum of the two dNSAF values. For clarity, only interactions captured in both RNase treated and non-treated purifications with less than 4-fold differences in relative abundance (i.e. 4 > dNSAFRNAse/dNSAFNon-treated >

0.25) have been included. In Supplemental Table 1 bait and prey proteins with similar profiles were manually grouped together. Proteins were grouped based on both the dNSAF values of each bait-prey pair, as well as the comparison of the relative abundance changes between RNase treated and non-treated samples. To visualize changes on a global level, heatmaps were generated from Supplemental Table 1 excluding ribosomal subunits. In the heatmaps red indicates high and yellow indicates low dNSAF values; black reflects lack of interaction under experimental conditions used.

RNA-Seq data analysis

Stranded RNA-Seq samples were barcode-separated and adaptor sequence 5′AGATCGGAAGAGCACACGTCTGAACTCCAGTCAC3′ removed using Trim-galore (http://www.bioinformatics.babraham.ac.uk/projects/trim_galore/) with the following parameters (-s 3 –e 0.3). To characterize the small RNA transcriptome, we employed Inchworm of Trinity (Release 2011-08-20) using default setting to perform *de novo* assembly of all transcripts identified in the previous step (Grabherr et al., 2011). Because Terminator-treated samples had less contamination from degraded transcripts, we used treated total mitochondrial RNA to build the transcriptome assembly. A custom script was used to remove potential one to two nt adaptor sequences that failed to be removed by Trim-galore. To eliminate contaminating nuclear-encoded RNAs, we removed the assembled transcripts if they mapped to the nuclear genome (http://tritrypdb.org, release 5.0) or to mitochondrial rRNA by the short read aligner BWA (version 0.5.8) (Li and Durbin, 2009). To evaluate similarity between terminator treated and untreated samples, read counts for each transcript were compared by Pearson correlation, and the

associated R-squared value was reported for each set of experiments. To predict candidate gRNAs, we extracted all assembled transcripts with a length equal to or shorter than 75 nt and mapped them to edited mitochondrial mRNA sequences. To perform the alignment allowing GU match, we developed a custom python script to generate alternative sequences of the original assembled transcripts by considering GU matches and mapped them to edited sequences by BWA using default settings. GU matches were considered to be equivalent to the canonical matches; we allowed one gap and up to three mismatches in our candidate gRNAs.

To analyze complex-bound RNAs, the trimmed complex-bound reads were mapped to the transcripts assembled from total mitochondrial RNA, and the read counts across all transcripts were summed in each sample. To identify the complex bound transcripts, a Fisher's exact test was used to assess whether a significantly higher proportion of complex-bound reads aligned to a given transcript than the proportion of total RNA reads. Transcripts with FDR $\leq$ 0.05, fold increase > 2, and a minimum of 2 supporting reads, were considered enriched. This analysis was performed using the average read counts of terminator treated and terminator untreated samples. The same analysis was repeated with individual replicates (+/- terminator treatment) separately and results between any two replicates were highly consistent with the average result. To cluster complexes based on similarity of enriched transcripts, we defined a transcript-by-complex matrix, with each matrix entry denoting the enrichment (1) or lack of enrichment (0) of a given complex (column) in a given transcript (row). Only transcripts found to be enriched in at least two complexes were included. We then performed hierarchical clustering of both the complexes and the transcripts using uncentered correlation-based distance measure and the *centroid linkage* agglomeration rule as implemented in Cluster 3.0

(http://bonsai.hgc.jp/~mdehoon/software/cluster/software.htm). The results were visualized using the Java TreeView package (Saldanha, 2004).

To test whether a complex showed an enriched binding at any given U-tail length, we compared the proportion of complex bound transcripts and proportion of total transcripts at each given U-tail length. Fisher's exact test was then applied to assess whether a significantly higher/lower proportion of complex bound transcripts was observed at any given U-tail length. We then $\log_2$ transformed the fold change of the enrichment results to generate the final plot.

Reference List

Aphasizhev,R. and I.Aphasizheva. 2007. RNA Editing Uridylyltransferases of Trypanosomatids. *Methods Enzymol.* **424**: 51-67.

Aphasizheva,I., D.Maslov, X.Wang, L.Huang, and R.Aphasizhev. 2011. Pentatricopeptide Repeat Proteins Stimulate mRNA Adenylation/Uridylation to Activate Mitochondrial Translation in Trypanosomes. *Mol. Cell* **42**: 106-117.

Fang,L., R.M.Kaake, V.R.Patel, Y.Yang, P.Baldi, and L.Huang. 2012. Mapping the protein interaction network of the human COP9 signalosome complex using a label-free QTAX strategy. *Mol. Cell Proteomics.* **11**: 138-147.

Grabherr,M.G., B.J.Haas, M.Yassour, J.Z.Levin, D.A.Thompson, I.Amit, X.Adiconis, L.Fan, R.Raychowdhury, Q.Zeng, Z.Chen, E.Mauceli, N.Hacohen, A.Gnirke, N.Rhind, P.F.di, B.W.Birren, C.Nusbaum, K.Lindblad-Toh, N.Friedman, and A.Regev. 2011. Full-length transcriptome assembly from RNA-Seq data without a reference genome. *Nat. Biotechnol.* **29**: 644-652.

Kaake,R.M., T.Milenkovic, N.Przulj, P.Kaiser, and L.Huang. 2010. Characterization of cell cycle specific protein interaction networks of the yeast 26S proteasome complex by the QTAX strategy. *J. Proteome. Res.* **9**: 2016-2029.

Koslowsky,D., Y.Sun, J.Hindenach, T.Theisen, and J.Lucas. 2013. The insect-phase gRNA transcriptome in Trypanosoma brucei. *Nucleic Acids Res.*

Li,H. and R.Durbin. 2009. Fast and accurate short read alignment with Burrows-Wheeler transform. *Bioinformatics.* **25**: 1754-1760.

Pelletier,M., L.K.Read, and R.Aphasizhev. 2007. Isolation of RNA Binding Proteins Involved in Insertion/deletion Editing. *Methods Enzymol.* **424**: 69-96.

Saldanha,A.J. 2004. Java Treeview--extensible visualization of microarray data. *Bioinformatics.* **20**: 3246-3248.

Zhang,Y., Z.Wen, M.P.Washburn, and L.Florens. 2010. Refinements to label free proteome quantitation: how to deal with peptides shared by multiple proteins. *Anal. Chem.* **82**: 2272-2281.